AN EXPERIMENTAL STUDY OF THE MOTORCYCLE
ROLL STABILIZATION TASK

David J. Eaton
Highway Safety Research Institute
The University of Michigan
Ann Arbor, Michigan

April, 1973

AN EXPERIMENTAL STUDY OF THE MOTORCYCLE
ROLL STABILIZATION TASK

## 1. INTRODUCTION

Although the literature concerning motorcycle and bicycle dynamics is not large, such research usually has been concerned with the uncontrolled single-track vehicle. The work of Sharp [1] represents the most complete theoretical analysis of the uncontrolled motorcycle presently available, and serves as a theoretical basis for the study described herein. Sharp's analysis included roll, yaw, lateral translation, and steering degrees of freedom, and the resulting equations are linear with constant coefficients. For use here, tire aligning moments due to tire sideslip have been added to Sharp's equations.

Of the few existing studies of a man and single-track vehicle as a closed-loop control system, the most significant are Van Lunteren, et al. (e.g., [2, 3]) and Weir [4]. While the former research represents a pioneering effort in obtaining rider transfer functions experimentally (with a bicycle simulator), it should be pointed out that Van Lunteren's major interest was the performance of the human operator under various conditions (drugs, etc.) and not the dynamics of the bicycle. Thus, the accuracy of the simulator dynamics with respect to real bicycles and the validity of the assumption of steering angle control (rather than steering torque) are questionable. On the other hand, the work of Weir, although strictly theoretical, was based upon the motion equations and motorcycle parametric data of Sharp, and represents a comprehensive study of the man-motorcycle system.

It is the purpose of the work described here to present experimental results and relate them to the theoretical studies of Sharp and Weir.

## 2. DESCRIPTION OF EXPERIMENTS

The particular rider task under consideration here is stabilization of the vehicle roll angle by means of steering torques applied to the handlebars. Path following and control by body movements are not being studied. From theoretical considerations, Weir [4] has shown that roll stabilization is best accomplished by steering torque control and that body lean control is more suited to the path following task. An "inner loop" of the multi-loop man/motorcycle control system postulated by Weir is shown in Figure 1, in which $\phi$ is the roll angle, $t_\delta$ is the rider-applied steering torque, i includes wind and road disturbances, and n is the rider's remnant. The block diagram of Figure 1 represents the man-motorcycle system model that is used in the present study.

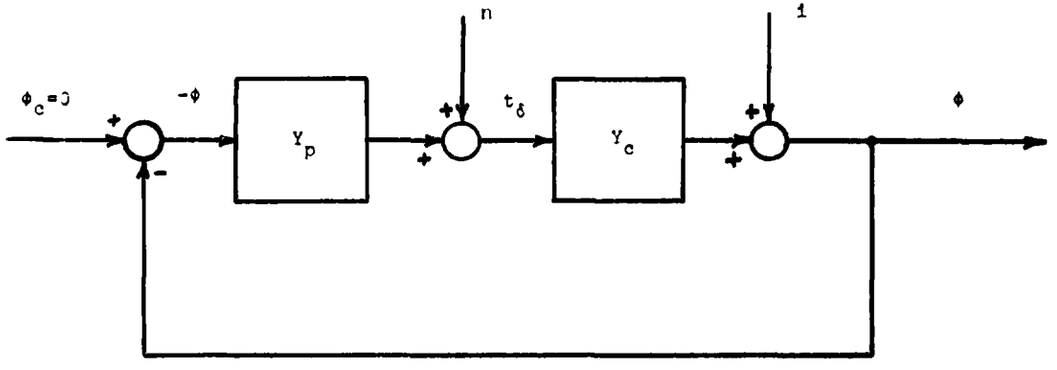


Figure 1. Block diagram of the man-motorcycle system.

The motorcycle transfer function, or controlled element, $Y_c(j\omega)$, can be calculated from the equations of motion of Sharp [1]. It will be shown that both $Y_c(j\omega)$ and the rider transfer function, $Y_p(j\omega)$, can also be obtained experimentally.

To restrict the experiments to the roll stabilization task, road tests were performed on a 0.5-mile section of essentially straight paved road in good condition. The test motorcycle was operated next to an automobile, which carried the power supplies and recording equipment. Figure 2 shows the experimental situation, including the rigid brace mounted on the motorcycle to reduce rider body lean, and the third wheel that was used to measure roll angle. (Also visible is a horizontal arm supporting two weights which was removed for these experiments.) Additional instrumentation included a rate gyro to sense roll rate, a steering angle potentiometer, and a strain-gaged bar to record steering torques. With this torque bar, it was necessary for the rider to steer with one hand. Throttle control was relocated to the rear frame. The effect of this unusual control arrangement upon the generality of the results is not known, but it is felt that any such effects were small and, at least, considerably smaller than they would have been if the rider had been using position control instead of torque control.

Three experienced riders, denoted Rider A, Rider B, and Rider C, were tested. These riders were chosen to be of approximately the same weight (170-196 lb.) to minimize changes in $Y_c(j\omega)$ due to variations in rider mass and mass distribution.

A total of fifteen experiments were performed with Rider A (the author). These experiments took place on two days about four months apart. On the first day, experiments began with a 30 mph test, followed by a 15 mph test, followed by a 30 mph test, etc., until eleven total were recorded, with three of each speed being suitable for analysis. The remaining nine tests were selected from a group of ten (all at 30 mph) performed on the second day.

On a single day, a total of thirteen tests were carried out with Rider B, with twelve of these being suitable for analysis. Similarly, on a single day, twelve tests were recorded with Rider C, eleven tests being suitable for analysis. Both riders were instructed to ride at a constant 30 mph while minimizing body movements with the aid of the brace attached to the motorcycle. A few practice runs were made before recording was begun.

The duration of each 30 mph test was about 50-60 seconds, while the 15 mph tests lasted about 65 seconds.

A major objective of the experiments was to identify the rider transfer function, $Y_p(j\omega)$. Since the wind/road disturbance i is unknown, it is necessary to estimate $Y_p(j\omega)$ by an open-loop method. To reduce bias errors arising from a correlation between n and $\phi$, a method developed by Wingrove and Edwards [5, 6, 7, 8] must be employed. When the remnant autocorrelation function is sufficently small for lags less than or equal to the rider's time delay, $\tau_p$, this method can remove most of the bias errors by first identifying $e^{\lambda j\omega}Y_p(j\omega)$, the transfer function having $-\phi(t-\lambda)$ as input and $t_\delta(t)$ as output, where $0 < \lambda \leq \tau_p$, since there is much less correlation between $\phi(t-\lambda)$ and $n(t)$ than between $\phi(t)$ and $n(t)$. The Wingrove-Edwards method must be coupled with an identification procedure that is constrained to identify only physically realizable systems. The impulse response method [6, 9], which first identifies a discrete form of the impulse response function of the unknown system, and then determines the transfer function by Fourier transformation, is such a procedure and has been used in this study.

## 3. DISCUSSION OF RESULTS

Preliminary analysis of the experimental data for 30 mph tests indicated that the theoretical controlled element, $Y_c(j\omega)$, could be accurately identified with the following relationship:

$$\hat{Y}_c(j\omega) = \frac{\hat{S}_{\phi t_\delta}(\omega)}{S_{t_\delta t_\delta}(\omega)}, \qquad (1)$$

where $\hat{Y}_c(j\omega)$ is the estimate of $Y_c(j\omega)$, $\hat{S}_{\phi t_\delta}(\omega)$ is the estimated cross-spectrum between $\phi$ and $t_\delta$, and $\hat{S}_{t_\delta t_\delta}(\omega)$ is the estimated power spectrum of $t_\delta$. An example of such an identification is shown in Figure 3. The theoretical $Y_c(j\omega)$, calculated from the equations of motion and the motorcycle parametric data measured for the test vehicle (Appendix A), is shown for comparison. The identification is seen to be the closest to the theoretical controlled element for frequencies of about 1-4 radians/second, where most of the power of the roll angle and steering torque records is located.

The fact that the theoretical $Y_c(j\omega)$ can be identified experimentally provides support for the motorcycle equations of motion and also indicates that the rider's remnant, n, is a much greater source of excitation to the man-machine system than the wind/road disturbance, i. When the remnant is the primary disturbance to the system, the Wingrove-Edwards method is required to identify $Y_p(j\omega)$.

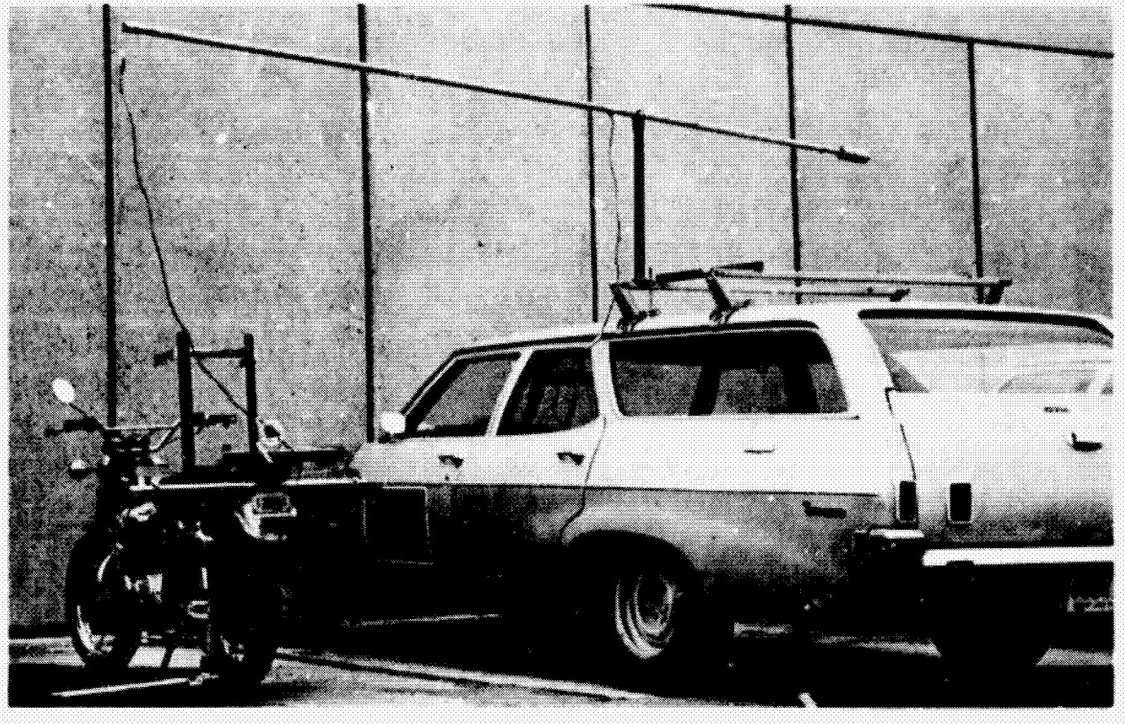

Figure 2. Test motorcycle and instrumentation car.

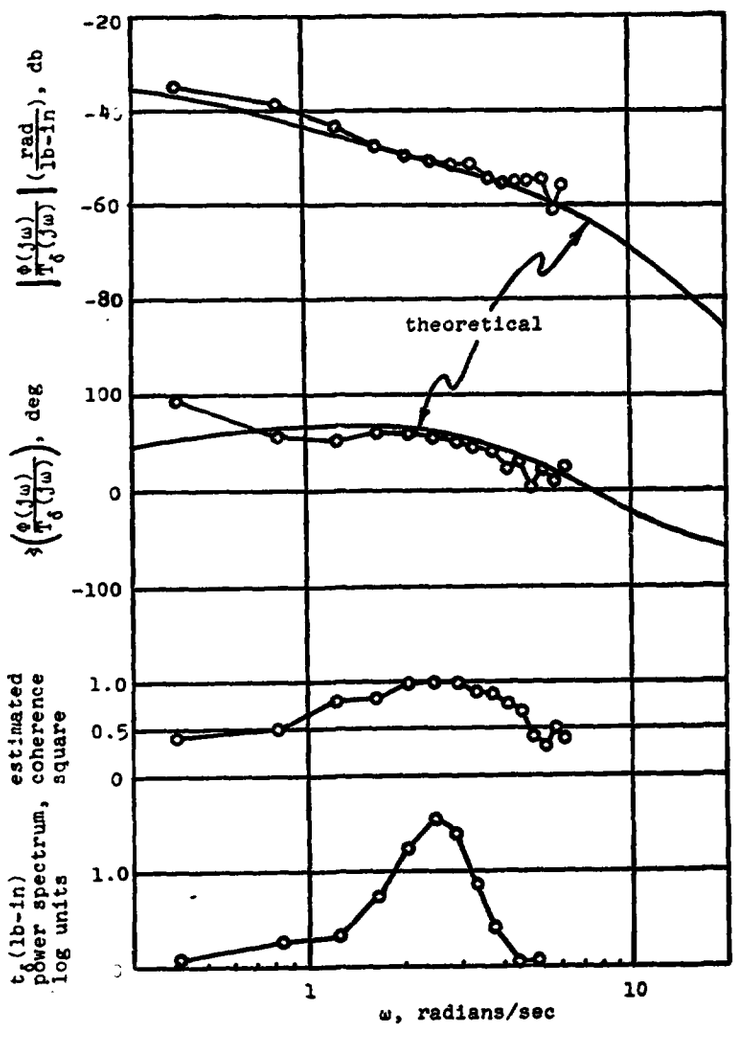


Figure 3. Identification of $Y_c(j\omega)$, 30 mph.

Since the impulse response and Wingrove-Edwards methods are not nearly as well documented in the literature as spectral analysis techniques, some rules regarding the interpretation of Bode diagrams of $\hat{Y}_p(j\omega)$ were derived from applying the methods to the identification of known systems from artificially created data, as outlined in Appendix B. A further aid to the interpretation of $\hat{Y}_p(j\omega)$ Bode diagrams was obtained by assuming the remnant power spectrum to be "white" and calculating the expected power spectrum of $t_\delta$, based on the estimate of $Y_p(j\omega)$ and the theoretical $Y_c(j\omega)$ (including the effect of the analog filter applied to the data).

Two example identifications of $Y_p(j\omega)$ are shown in Figure 4. In general, the form of $Y_p(j\omega)$ for the 30 mph tests was found to be

$$Y_p(j\omega) = -K_p e^{-\tau_p j\omega}(T_\ell j\omega + 1). \qquad (2)$$

The value of $T_\ell$ was negligibly small, except for the tests carried out with Rider A on the second day. Thus, for most of the 30 mph tests, a rider transfer function of the form,

$$Y_p(j\omega) = -K_p e^{-\tau_p j\omega}, \qquad (3)$$

fits the data. In the three 15 mph tests the rider transfer function was of the form

$$Y_p(j\omega) = -K_p\, j\omega\, e^{-\tau_p j\omega}(T_\ell j\omega + 1). \qquad (4)$$

Estimated mean values of the parameters in Equations (2-4) are presented in Table 1. The confidence intervals for the true mean values were calculated on the assumption that the estimates of the means were unbiased. Since this assumption may not be valid, more certainty may be attached to the width of the confidence interval than its midpoint.

The resulting rider transfer functions were found to be consistent with the crossover model, which was employed by Weir [4] in his theoretical analysis of the man-motorcycle system. The crossover model requires that

$$Y_p(j\omega)Y_c(j\omega) \doteq \frac{\omega_c e^{-\tau_e j\omega}}{j\omega}, \quad \omega \doteq \omega_c,$$

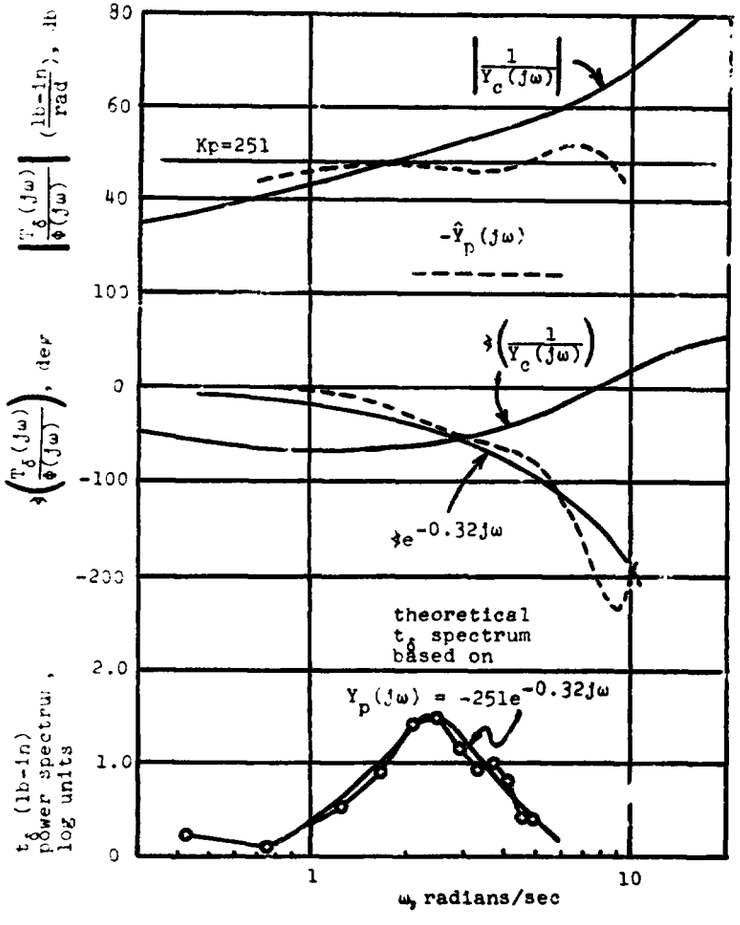


Figure 4a. Identification of $Y_p(j\omega)$ for a single test (Rider $^pA$, 30 mph, first day).

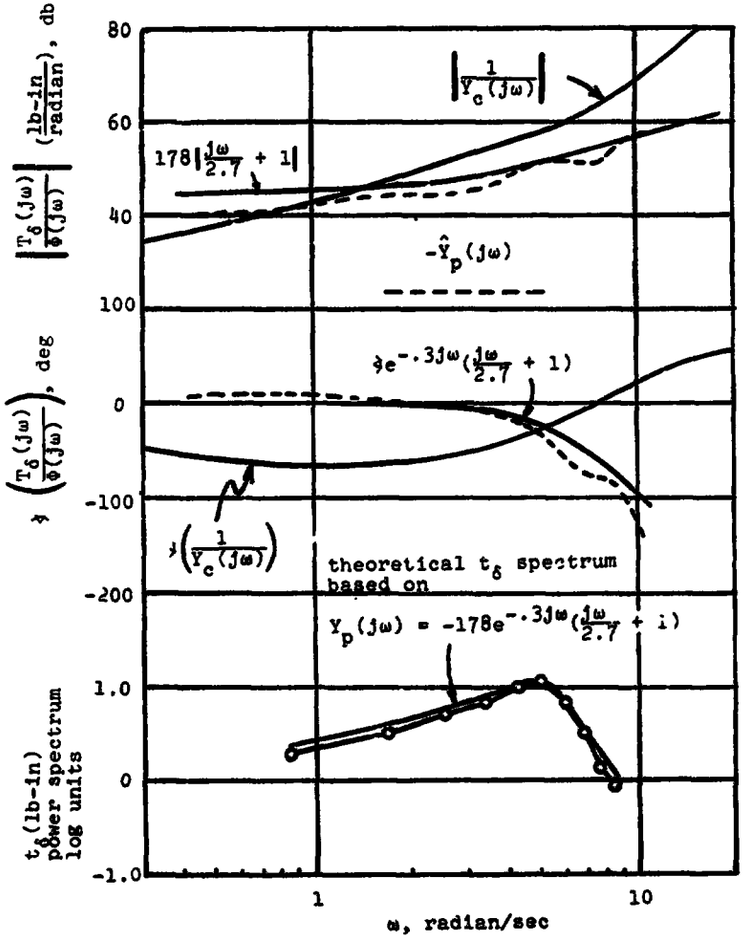


Figure 4b. Identification of $Y_p(j\omega)$ for a single test (rider A, 30 mph, second day; the case in which $\hat{Y}_p$ evidenced the most lead).

TABLE 1

SUMMARY OF RIDER TRANSFER FUNCTIONS

| | Day of Test | 1 | 1 | 2 | 3 | 4 |
|---|---|---|---|---|---|---|
| | Speed, mph | 15 | 30 | 30 | 30 | 30 |
| | Rider | A | A | A | B | C |
| | Form of $\hat{Y}_p(j\omega)$ | $-K_p j\omega e^{-\tau_p j\omega} \cdot (T_\ell j\omega + 1)$ | $-K_p e^{-\tau_p j\omega}$ | $-K_p e^{-\tau_p j\omega} \cdot (T_\ell j\omega + 1)$ | $-K_p e^{-\tau_p j\omega}$ | $-K_p e^{-\tau_p j\omega}$ |
| Mean Values of Estimated Quantities | $K_p$, $\frac{\text{lb-in}}{\text{radian}}$ | 75.6 | 277 | 261 | 167 | 206 |
| | $\tau_p$, seconds | 0.300 | 0.298 | 0.300 | 0.328 | 0.299 |
| | $1/T_\ell$ $\frac{\text{radians}}{\text{second}}$ | 9.04 | | 6.45 | | |
| | $\phi_m$, degrees | 25 | 28.3 | 48.6 | 41.4 | 39.1 |
| 90% Confidence Intervals | $K_p$, $\frac{\text{lb-in}}{\text{radian}}$ | (53.6, 97.6) | (219, 335) | (236, 286) | (152, 182) | (185, 227) |
| | $\tau_p$, seconds | (.216, .384) | (.260, .336) | | (.287, .369) | (.276, .322) |
| | $1/T_\ell$ $\frac{\text{radians}}{\text{second}}$ | (3.37, 11.42) | | (5.27, 7.41) | | |
| | $\phi_m$, degrees | | (15.2, 41.4) | (42.4, 54.8) | | (36.7, 41.5) |
| Parameters for Cross-over Model, Based on Average $\hat{Y}_p(j\omega)$ | $\omega_c$, $\frac{\text{radians}}{\text{seconds}}$ | 3.2 | 2.0 | 1.9 | 1.3 | 1.5 |
| | $\tau_e$, seconds | 0.370 | 0.533 | 0.393 | 0.572 | 0.533 |

where $\omega_c$ is the crossover frequency. Figure 5 shows a Bode diagram of $\bar{Y}_p(j\omega)Y_c(j\omega)$, where $\bar{Y}_p(j\omega)$ is the average of the estimated rider transfer functions from the second test day (from Table 1), and a Bode diagram of $\bar{Y}_p(j\omega)\bar{Y}_c(j\omega)$ for the 15 mph tests. In the 15 mph situation, it was necessary to use the average of $Y_c(j\omega)$, as estimated from Equation (1), because there was noticeably less agreement between the theoretical $Y_c$ and the experimental $Y_c$, as compared with the 30 mph tests. It can be seen that, with appropriate values of $\omega_c$ and $\tau_e$, the crossover model closely fits the experimental results near the crossover frequency. The values of $\omega_c$ and $\tau_e$ that were selected for each group of data are included in Table 1.

As shown in Figure 3, $|Y_c(j\omega)|$ at 30 mph has a broad region of a -20 db/decade slope, with a steeper drop-off near 9 radians/second. As speed decreases, this drop-off moves to lower frequencies. Thus, to fit the crossover model, increasing amounts of lead equalization are required as speed decreases. At 30 mph, however, lead is optional.

Estimates of the remnant power spectra were made from the estimated rider impulse response functions. These calculated spectra, which, precisely speaking, were based on the estimates of $Y_p(j\omega)$ before they were fitted by Equations (3-4), were generally of the form

$$S_{nn}(\omega) \doteq \frac{\text{Constant}}{25 + \omega^2} ,$$

the form that would be obtained if "white" noise were passed through a first order filter having a break frequency of 5 radians/second, which, in fact, was the filter applied to the data before digitizing. Thus, to at least about 10 radians/second, the actual unfiltered remnant is apparently "white", as was assumed earlier.

The estimated remnant consists of all the steering torque output of the rider that is not related to the roll angle by the linear transfer function $-Y_p(j\omega)$. The remnant contains (1) rider output which is nonlinearly related to the roll angle, (2) path correction steering torques not linearly related to the roll angle (such as corrections needed due to the real road not being perfectly straight, obstacle or bump avoidance, etc.), (3) miscellaneous steering torques, voluntary or involuntary (including direct mechanical transmission of road shocks through the rider's arms to the handlebars, although road shocks are high frequency phenomena and would not be included in the estimated remnant), (4) any time variation in $Y_p(j\omega)$, and (5) errors in identifying $Y_p(j\omega)$. Since the rider is using torque control for purposes other than roll stabilization, it was found that the mean square remnant was a large proportion of the mean square steering torque: from 30-95%. It is

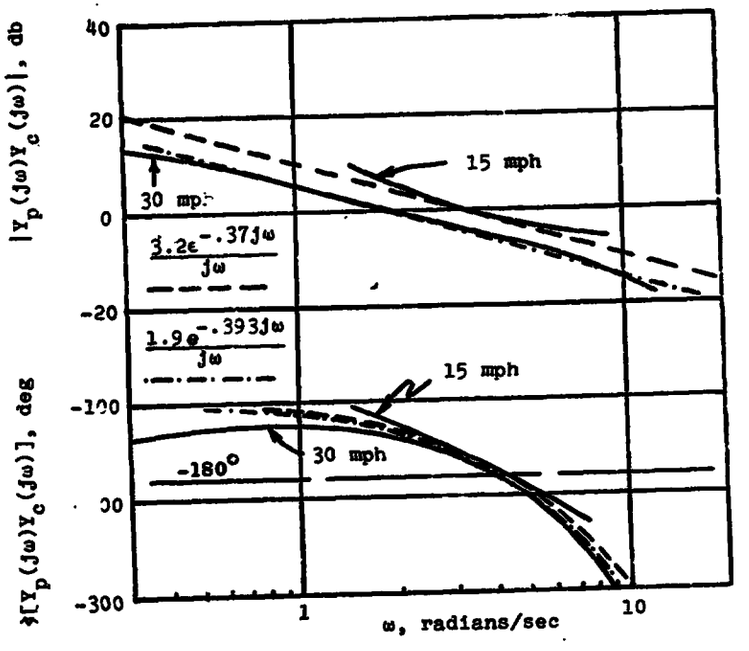


Figure 5.

Crossover model approximations to $\bar{\bar{Y}}_p(j\omega)Y_c(j\omega)$ (rider A, 30 mph, second day average, $\bar{\bar{Y}}_p(j\omega) = -2.1e^{-.3j\omega}(\frac{j\omega}{6.45} + 1)$), and $\bar{\bar{Y}}_p(j\omega)\bar{\bar{Y}}_c(j\omega)$ (rider A, 15 mph, first day average, $\bar{\bar{Y}}_p(j\omega) = -75.6j\omega e^{-.3j\omega}(\frac{j\omega}{9.0} + 1)$).

not known how much of this is due to errors in estimating $Y_p(j\omega)$. Probably the identification errors increased with the remnant, since a large remnant tended to make accurate identification of $Y_p(j\omega)$ more difficult.

## 4. CONCLUSIONS

1. During normal operation on a paved road in good condition, the primary excitation to the man-motorcycle system is the rider's "remnant". This fact allows accurate identification of the controlled element ($Y_c(j\omega)$) by open-loop cross-spectral analysis, at least for the frequency range in which there is substantial amplitude of the records being analyzed. Agreement between the theoretical and experimental $Y_c(j\omega)$ is better at 30 mph than at 15 mph.

2. The Wingrove-Edwards method [5] can be used to identify $Y_p(j\omega)$, the transfer function of the rider for the task studied. The experimental steering torque power spectra were helpful in interpreting Bode diagrams of $Y_p(j\omega)$.

3. At 30 mph, the rider transfer function $Y_p(j\omega)$ was found to be a constant gain and time delay, with the optional inclusion of lead equalization having a break frequency in the neighborhood of 5-10 radians/sec. Time delays were about 0.3 second for all the tests, and gains were about 250-350 lb-in/radian.

4. Only three experiments were performed at 15 mph, but the results of these indicated that a combination of rate control and lead equalization (break frequency, 5-10 radians/second) was required on the part of the rider. Here the time delays were about 0.25-0.35 second, and the gains were about 60-90 lb-in/radians.

5. The experimental results agree with the crossover model, which has been used to theoretically study the man-motorcycle system [4].

6. Most of the rider's steering torque output was remnant. The power spectrum of n(t) was found to have about the same shape as that of "white" noise passed through the same filter that was applied to the original analog records.

## REFERENCES


1. Sharp, R.S., "The Stability and Control of Motorcycles," Journal Mechanical Engineering Science, Vol. 13, No. 5, 1971.

2. Van Lunteren, A., and Stassen, H.G., "Investigations on the Characteristics of a Human Operator Stabilizing a Bicycle Model," Intern. Symp. on Ergonomics in Machine Design, Prague, 1967.

3. Van Lunteren, A., and Stassen, H.G., "On the Variance of the Bicycle Rider's Behavior," 6th Annual Conference on Manual Control, Wright Patterson AFB, Ohio, 1970.

4. Weir, D.H., "Motorcycle Handling Dynamics and Rider Control and the Effect of Design Configuration on Response and Performance," Ph.D. Thesis, University of California (L.A.), 1972.

5. Wingrove, R.C., and Edwards, F.G., "Measurement of Pilot Describing Functions from Flight Test Data with an Example from Gemini X," 4th Annual NASA - University Conference on Manual Control, The University of Michigan, March 1968.

6. Wingrove, R.C., and Edwards, F.G., "A Technique for Identifying Pilot Describing Functions from Routine Flight-Test Records," NASA TN D-5127, May 1969.

7. Wingrove, R.C., "Comparison of Methods for Identifying Pilot Describing Functions from Closed-Loop Operating Records," NASA TN D-6235, March 1971.

8. Edwards, F.G., "Determination of Pilot and Vehicle Describing Functions from the Gemini-10 Mission," NASA TN D-6803, May 1972.

9. Taylor, L.W., Jr., "A Comparison of Human Response Modeling in the Time and Frequency Domains," Third Annual NASA-University Conference on Manual Control, University of Southern California, L.A., March 1-3, 1967.

10. Jenkins, G.M., and Watts, D.G., Spectral Analysis and Its Applications. Holden-Day, San Francisco, 1969.

## APPENDIX A

## MEASUREMENT OF MOTORCYCLE PARAMETERS

To calculate the theoretical $Y_c(j\omega)$ from the motorcycle equations of motion [1], it was necessary to make a number of measurements of the test vehicle.

In addition to geometric measurements, mass and mass distribution estimates were made for the front wheel, fork and handlebar assembly, and the total motorcycle with Rider A in place on the seat. (The brace in Figure 2 was used.) The following quantities were measured:

1. Masses
2. Center of gravity locations
3. Roll moments of inertia (x-axis)
4. Yaw moments of inertia (z-axis)
5. XZ products of inertia

It was necessary to attach the front frame assembly and the entire vehicle to fixtures to measure mass distribution. Moments of inertia were measured with cable-suspended torsional pendula, except for the roll moment of inertia of the man-motorcycle combination, for which measurements were made by swinging the assembly on knife edges.

Additionally, wheel polar moments of inertia were measured with a torsional pendulum arrangement. An effective polar moment of inertia for the engine and transmission was calculated from data supplied by the manufacturer.

Tire properties were obtained from the HSRI flat bed tire tester. Measurements included the dependence of tire lateral force and aligning moments on slip and inclination angles, and the tire relaxation length.

Friction in the steering head was estimated and found to be negligible, on the basis of analog computer studies not discussed here.

## APPENDIX B

## IDENTIFICATION OF KNOWN TRANSFER FUNCTIONS

Artificial data were prepared by digital computer as follows: a subroutine generated a series of random numbers $z(kh)$, $k=1,2,\ldots 500$, $h=0.1$ second, where $z(kh)$ was normally distributed with mean zero. The artificial remnant was calculated from

$$n(kh) = \alpha_1 n[(k-1)h] + z(kh), \quad k=1,2,\ldots 500$$

The theoretical autocorrelation function of $n(kh)$ is [10]

$$r_{nn}(k'h) = \alpha_1^{|k'|}, \quad k'=0,\pm 1,\pm 2,\ldots \ .$$

The "rider" and "motorcycle" transfer functions were taken to be

$$Y_{p_1}(j\omega) = e^{-0.4j\omega},$$

$$Y_{p_2}(j\omega) = 1.5e^{-0.4j\omega},$$

and

$$Y_c(j\omega) = \frac{1}{j\omega} \ .$$

The degree of bias in estimating $Y_p(j\omega)$ by the Wingrove-Edwards method is increased by increasing $r_{nn}(\tau_p) = r_{nn}(0.4)$ [5], or, in this case, by increasing $\alpha_1$. Zero bias results if $r_{nn}(\tau)=0$ for $\tau > 0.4$.

Figure 6 shows the identification of $Y_{p_1}$ when $\alpha_1 = 0.3$ ($r_{nn}(0.4) = .0081$) and $Y_{p_2}$ when $\alpha_1 = 0.8$ ($r_{nn}(0.4) = 0.41$). In general, $|\hat{Y}_{p_2}|$, which is more biased, tends more toward $1/Y_c(j\omega)$ at the higher and lower frequencies than $|\hat{Y}_{p_1}|$. Further, $\angle(Y_{p_2})$ is underestimated for $\omega > 2$ radians/second. If the bias is increased further, it has been found that both $|\hat{Y}_p|$ and $\angle(Y_p)$ tend to be underestimated. On the other hand, it is seen that $|\hat{Y}_{p_1}|$ and $\angle(\hat{Y}_{p_1})$, which should not be strongly biased, tend to be slightly overestimated.

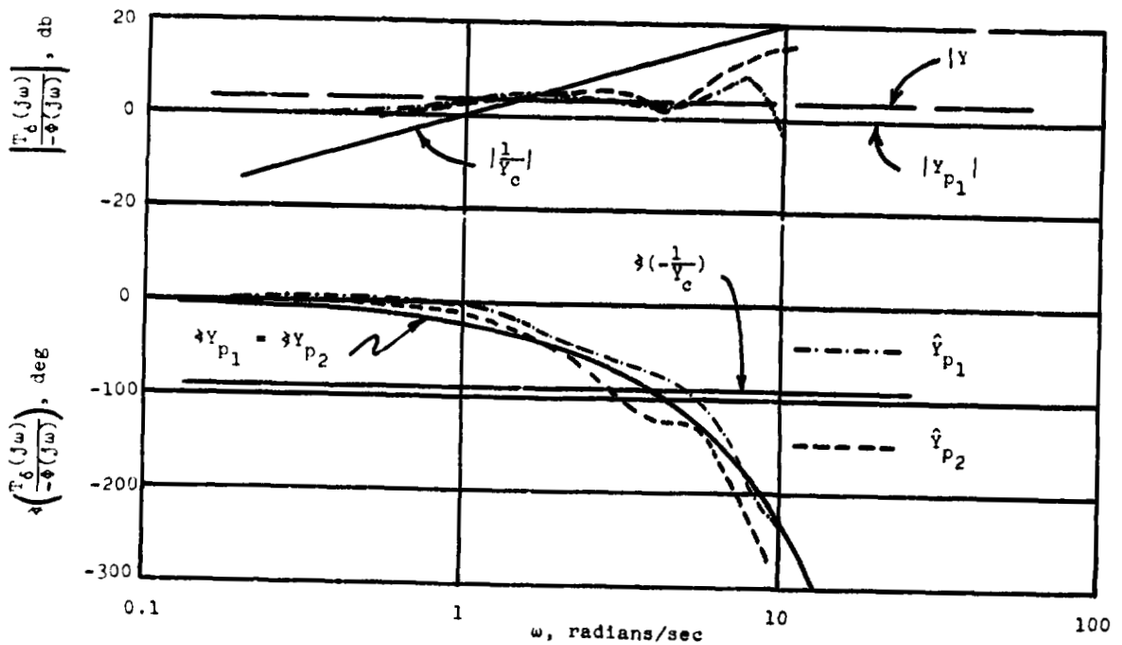


Figure 6. Identification of known "rider" transfer functions from artificial data by the time shifting method.